COMPARISON IN THE HAUSDORFF METRIC OF RECONSTRUCTION OF 3D URBAN TERRAIN BY FOUR PROCEDURES

Dimitri Bulatov
Fraunhofer Institute of Optronics, System Technologies and Image Exploitation
Gutleuthausstrae 1, 76275 Ettlingen, Germany

John Lavery
Mathematics Division, Army Research Laboratory, P.O. Box 12211, Research Triangle Park, NC 27709-2211, U.S.A.

Keywords: 3D, Alpha shapes, Cubic spline, Hausdorff distance, Irregular data, Iso-surface, L_1 spline.

Abstract: We computationally compare four procedures, namely, alpha-shapes, iso-surface extraction, gridfit and L_1 splines for geometric reconstruction of 3D urban structures represented by irregular point clouds with abrupt changes in density. For significant numbers of outliers, L_1 splines produce the most accurate reconstructions both visually and when measured analytically in the Hausdorff metric but are more computationally expensive than the other three procedures.

1 INTRODUCTION

Obtaining textured surfaces from point clouds retrieved by passive sensors is a topic of increasing interest in computer vision and its applications, such as automatic navigation and surveillance. Point clouds obtained by photogrammetric methods are commonly irregular and have abrupt changes of density because the regions with high density of points resulting from patches of good local coverage and textured areas are interspaced with large patches of poor coverage. The abruptly changing density of the point clouds that we consider here is in contrast to the roughly uniform density of the point clouds obtained, for example, from local LIDAR scanning of objects, for which theoretically established conditions that guarantee reconstruction of a topologically correct surface with error bounds are known (Amenta et al., 2000). In addition to the irregular density, point clouds produced from light, inexpensive cameras, especially from cameras without internal navigation capabilities, have a high level of noise and a significant number of outliers, i.e., points far from the surface resulting, for example, from small moving objects, occlusions, or spurious matches in the areas of roughly homogeneous intensity distribution which are, in general, not easy to eliminate in the preprocessing step. In some cases, it is possible to cope with these negative properties using model assumptions, for example, the local 2.5D character of digital terrain maps (DTMs), which enables extraction of roof planes (Haala N., 1998) and piecewise planar structures in general (Mayer H., 2006), but, in general, robust algorithms for reconstruction of 3D surface for various topological types are not yet available and are therefore widely investigated. In this context, numerous procedures have been considered over the past two decades, including alpha shapes (α-shapes) (Edelsbrunner and Mücke, 1994), TMSs (triangular mesh surfaces, called in the 2.5D case triangulated irregular networks or, for short, TINs) (Boissonnat et al., 2006), iso-surface extraction (Kazhdan, 2005; Hoppe et al., 1992), polynomial splines (Eck and Hoppe, 1996), L_1 splines (Bulatov and Lavery, 2010; Lavery, 2001; Lin et al., 2006) and gridfit, a widely used modeling tool available in MATLAB (D'Errico, 2006).

In this paper, we will investigate the relative accuracy of the surfaces produced by α-shapes, iso-surface extraction, gridfit and L_1 splines.

These comparisons follow on and extend previous work on comparison of α-shapes with conven-

Bulatov D. and Lavery J. (2010).
COMPARISON IN THE HAUSDORFF METRIC OF RECONSTRUCTION OF 3D URBAN TERRAIN BY FOUR PROCEDURES.
In *Proceedings of the International Conference on Computer Graphics Theory and Applications*, pages 125-129
DOI: 10.5220/0002764501250129

tional splines and L_1 splines (Bulatov and Lavery, 2009). While in (Bulatov and Lavery, 2009) the emphasis was on procedures that handled all steps of the process from video as input to textured geometric models as output and merely visual comparison of reconstruction results was the objective, the present paper focuses on the geometric reconstruction portion of this process and its quantitative evaluation. This portion starts from a given cloud of points or (oriented) patches and ends up with a 3D triangular mesh. We choose an artificially constructed object as the basis for comparison so that ground truth is available. The standard deviation of Gaussian noise and the outlier percentage is varied. Deviation of the reconstructed surface from ground truth will be measured not by orientation-dependent classical error measures such as root-mean-square, but rather by the orientation-independent Hausdorff metric. We assume here knowledge of a 2D (u,v)-parametrization of a given point cloud $S = \{\mathbf{x}^m = (x^m, y^m, z^m),\ m = 1,2,\ldots,M\}$, from which the object is to be reconstructed.

In Section 2, we describe the Hausdorff metric in which the comparisons will be carried out and the four procedures that will be compared. Computational results are presented in Section 3. Concluding remarks and discussion of future research are given in Section 4.

2 HAUSDORFF METRIC AND RECONSTRUCTION PROCEDURES

In this section, we outline and motivate our choice of the Hausdorff metric in which the comparisons will be carried out and give brief descriptions of the four procedures that will be compared, namely, α-shapes, iso-surface extraction, gridfit and L_1 splines.

2.1 Hausdorff Metric

A fundamental issue when making comparisons is the metric (measure of similarity) in which the comparisons are made. Conventional metrics such as rms (root mean square—the square root of the average error) and generalizations thereof, such as the L_p norms (DiBenedetto, 2002), measure similarity in ways inconsistent with human perception. For many commonplace situations, including, for example, thin walls in urban terrain, these metrics indicate that two sets are nearly the same when observers judge them to be dissimilar. In order to measure *completeness* and *correctness* (Heipke et al., 1997) of a geometric reconstruction (Seitz et al., 2006), it is now common to use (generalizations of) the Hausdorff metric (Olson and Huttenlocher, 1997). The Hausdorff metric is sensitive to outliers, a property that makes it a suitable tool for evaluating surface reconstruction methods for practical applicability such as automatic navigation. In our case, the outliers are not input sample points but triangles of the resulting mesh that contain points far from the surface. Some generalizations of the Hausdorff metric play down the effect of outliers (Baddeley, 1992), but in this paper we shall adopt the original Hausdorff metric to perform the comparisons. We denote the distance from point $\mathbf{x}$ to mesh $\mathcal{Y}$ and the distance from mesh $\mathcal{X}$ to mesh $\mathcal{Y}$ by $d(\mathbf{x},\mathcal{Y}) = \inf_{\mathbf{y}\in\mathcal{Y}} d(\mathbf{x},\mathbf{y})$ and $d(\mathcal{X},\mathcal{Y}) = \sup_{\mathbf{x}\in\mathcal{X}} d(\mathbf{x},\mathcal{Y})$, respectively. For our purposes, $d(\mathbf{x},\mathbf{y})$ is the Euclidean distance between $\mathbf{x}$ and $\mathbf{y}$. The Hausdorff metric for the "distance" from $\mathcal{X}$ to $\mathcal{Y}$ is

$$d_H(\mathcal{X},\mathcal{Y}) = \max\{d(\mathcal{X},\mathcal{Y}), d(\mathcal{Y},\mathcal{X})\}. \qquad (1)$$

If $\mathcal{Y}$ is the ground-truth mesh, then the first term in (1) denotes correctness and the second term completeness of the reconstruction. Effective algorithms are needed for estimating $d(\mathcal{X},\mathcal{Y})$ on the triangular meshes considered here. We implemented the main features of the method of (Guthe M., 2005), which uses octrees for coarse identification for a given vertex $\mathbf{x}$ of the mesh $\mathcal{X}$ the part $\mathcal{Y}' \subseteq \mathcal{Y}$ to which computing distance makes sense. Then we performed fast computation of distance from $\mathbf{x}$ to every vertex, edge and face of $\mathcal{Y}'$. The minimum of these distances is an estimate of $d(\mathbf{x},\mathcal{Y})$.

2.2 Alpha Shapes

Alpha shapes is the well known method introduced in (Edelsbrunner and Mücke, 1994). Given a point sample S, a triangle formed from a triple of points is added to the list of triangles if no point of S lies in one of two open balls of radius α around these points. Clearly, for very small α, the α-shape will be S itself and, for $\alpha \to \infty$, the convex hull of S will be obtained. Since α-shapes are subsets of Delaunay triangulations, their computation can be performed rather fast. Another advantage of α-shapes is that they provide 3D models without needing parametrization. On the other hand, the procedure is not robust against outliers.

2.3 Iso-surface Extraction

The iso-surface extraction procedure that we use in this paper is that given in (Kazhdan, 2005). Given

a closed surface $\mathcal{F}$, the procedure first retrieves the Fourier transform of the characteristic function ($\chi(\mathbf{x}) = 1$ if $\mathbf{x} \in \mathcal{F}$ and $\chi(\mathbf{x}) = 0$ if $\mathbf{x} \notin \mathcal{F}$) from the point set S and the set of oriented normal vectors using Stokes's theorem (see (Kazhdan, 2005) for more details). Then it obtains an implicit function that represents the surface by setting $\chi(\mathbf{x}) = c$ where c is suitable constant. Finally, it performs meshing using a marching cubes algorithm (Lorensen and Cline, 1987). This procedure has the advantages of not requiring a parametrization and of being able to obtain the normal vectors and their orientations from the camera trajectory.

2.4 Gridfit

Gridfit in its standard implementation is an approximation procedure for fitting 2.5D surfaces (D'Errico, 2006). We use gridfit to generate 3D parametric surfaces of the form $(x(u,v), y(u,v), z(u,v))$, where x, y and z are 2.5D surfaces with respect to (u,v). Gridfit solves a least-squares system of the type

$$(1-\lambda)||A\mathbf{x}-b||_2^2 + \lambda||B\mathbf{x}||_2^2, \qquad (2)$$

where the first term is the data fitting term and the second term is the regularization term. The parameter λ determines the balance between accurately fitting the data (small λ) and smoothing out the surface (large λ). The version of gridfit used in this paper constructs a C^0 surface that fits the data approximately linearly on triangles and regularizes the surface by approximate equalization of the partial derivatives at the vertices of the triangles.

2.5 L_1-splines

Reconstruction with L_1 splines was described in (Bulatov and Lavery, 2010). Let (u^m, v^m) be the parametric postion of (x^m, y^m, z^m). The key idea is to minimize a functional that consists of

$$(1-\lambda)\sum_{m=1}^{M}|z(u^m,v^m)-z^m| + \qquad (3)$$
$$\lambda\int_D (|z_{uu}|+2|z_{uv}|+|z_{vv}|)\,du\,dv + \varepsilon\sum_{nodes}(|z_u|+|z_v|)$$

and 12 analogous expressions involving x, y and z over the manifold of cubic L_1 splines, that is, C^1-smooth piecewise cubic functions x, y and z on a given (u,v)-grid. Similar to (2), the first term in (3) expresses how closely the data points are fitted, the second term expresses, by minimizing absolute values of second partial derivatives, how close the surface is to a piecewise planar surface and the last term prevents it from having a non-unique minimum. Just as was the case for gridfit, the balance parameter λ determines the trade-off between fitting the data and smoothing the surface. The third term prevents the functional from having a non-unique minimum, and so any sufficiently small, positive number can be taken for ε. As in gridfit, the resulting mesh is formed by connecting the neighboring spline knots.

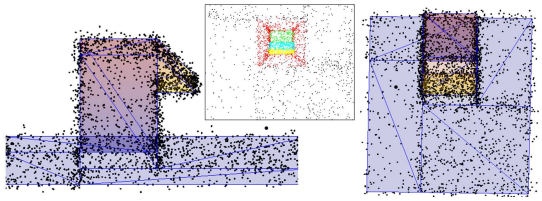

Figure 1: Model "house with overhanging roof" and point cloud with no outliers. Left: view from side, right: view from top, middle at top: parametrization in (u,v)-domain (points on the ground, on the walls, on the horizontal, upper and lower overhanging parts of the roof are marked in black, red, green, cyan and yellow, respectively).

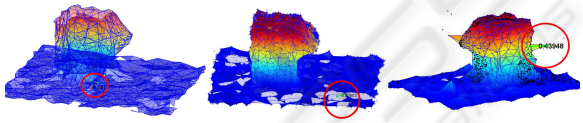

Figure 2: Surfaces extracted by α-shapes. Noise level 0.05 everywhere. Left and center: no outliers. Left: $\alpha = 5\cdot 10^4\sigma$, center: $\alpha = 2\cdot 10^4\sigma$. Right: outlier percentage 0.01, $\alpha = 5\cdot 10^4\sigma$.

3 COMPUTATIONAL RESULTS

The test object represented by the point cloud S must be simple enough that it can be correctly evaluated with the Hausdorff metric. On the other hand, S must possess all properties of a point cloud obtained by photogrammetric methods in urban terrain: gradient discontinuities (characteristic for manmade objects), high Gaussian noise, several outliers and varying density of points. In this paper, the point cloud S to be used in the comparisons represents a house with an overhanging roof (see Figure 1). The experiments were carried out for levels 0.01 and 0.15 of Gaussian

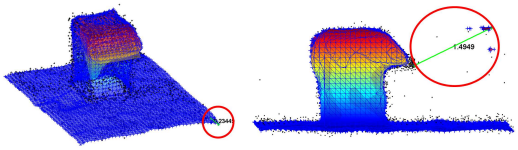

Figure 3: Surfaces produced by iso-surface extraction. Left: outlier percentage 0.0, right: outlier percentage 0.01.

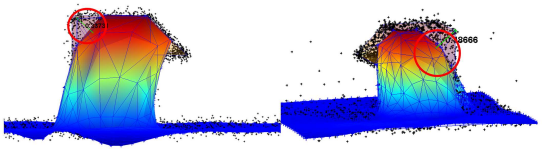

Figure 4: Gridfit surfaces. Outlier percentage is 0.01 everywhere. Equally spaced grid. Left: $\lambda = 0.2$, right: $\lambda = 0.33$.

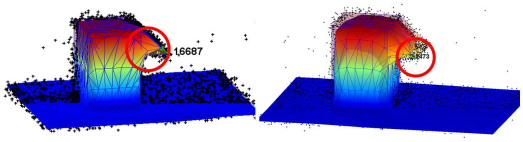

Figure 5: L_1 splines. Outlier percentage is 0.01 everywhere. Equally spaced grid. Left: $\lambda = 0.3$, right: $\lambda = 0.5$.

noise and for percentages 0%, 1% and 10% of outliers (i. e. points randomly chosen in the bounding box of the object) for x, y, z coordinates of the point (in the case of iso-surface extraction also for normal vectors). The density of points remained unchanged in all experiments but was variable in different regions of the data set. For each level of noise and outliers, we carried out data-set generation, reconstruction and evaluation 10–15 times and computed the average of the Hausdorff distances according to (1).

In the α-shapes procedure, we used $\alpha = 2 \cdot 10^4 \sigma$ and $5 \cdot 10^4 \sigma$, values that produce the best results for the point clouds of interest here. Here, σ is the standard deviation of the data-set coordinates. The results are shown in Figure 2. Here and in what follows, the point $\mathbf{x}$ on the approximating surface that yields the value of the Hausdorff metric (the maximum distance from the approximating surface to the ground-truth mesh) is at the center of a red circle and a green line is drawn from $\mathbf{x}$ to the closest point on the house model.

Table 1: Hausdorff-metric errors for the surfaces of Figures 2–5. Explanation about choice of parameters is given in Sec. 2 and Sec. 3. The computing times are approximate, since the algorithms were implemented in different programming languages and average correction factors were applied.

method	noise	outl. (%)	parameters	Hausdorff -distance	comp. time
α-shapes	0.01	0.00	$\alpha = 2 \cdot 10^4 \sigma$	0.26030	$\approx$ 2.0 sec.
	0.05			0.27441	
	0.01	0.00	$\alpha = 5 \cdot 10^4 \sigma$	0.22844	
	0.05			0.30783	
iso-surface	0.05	0.00		0.17134	$\approx$ 4.5 sec.
		0.01		0.85048	
gridfit eq. spaced	0.05	0.00	$\lambda = 0.2$	0.20819	$\approx$ 1 sec.
		0.01		0.38543	
		0.1		0.66349	
		0.00	$\lambda = 0.33$	0.26813	
		0.01		0.35752	
		0.1		0.53354	
L_1-splines	0.05	0.00	$\lambda = 0.3$	0.19457	$\approx$ 240 sec.
		0.01		0.19387	
		0.1		0.45619	
		0.00	$\lambda = 0.5$	0.26196	
		0.01		0.24133	
		0.1		0.30898	

For iso-surface extraction, we consider the fact that the result must be a closed surface and exclude from consideration all triangles that lie outside of the bounding box of the object. The bandwidth of the reconstruction (given by the voxel-grid for calculating forward and inverse FFT) was chosen to be 64. The orientation of the normals on points for the data set described were computed according the position of each point (on the ground, at the walls, on the roof, on the underside of the overhang). The computational results are presented in Fig 3.

For gridfit and L_1 splines, we generated surfaces $x(u,v), y(u,v), z(u,v)$ on the (u,v) domain $[-1.15, 2.15] \times [-2.15, 2.15]$. The (u,v)-parametrization is depicted on the right in Figure 1. Although a robust iterative procedure of generating parametrized data sets from similar point clouds is given in (Bulatov and Lavery, 2010), for the present paper, we chose manually suitable spatial homographies for points on the ground, at the walls and on the roof and under the overhang that transform the points from different parts of the house into the (u,v)-plane and preserve topological relations between these points. Both surfaces were computed for 50×50 equally spaced rectangular (u,v)-grids and reasonable balance parameters $\lambda = 0.2$ and 0.33 for gridfit and $\lambda = 0.3$ and 0.5 for L_1 splines. Figure 4 shows the gridfit reconstruction with different balance parameters. The reconstructions with L_1 splines are given in Figure 5. In Table 1, we present the average Hausdorff-metric errors between the reconstructions in Figures 2–5 and the ground truth. As Figures 2–5 and Table 1 indicate, the α-shapes and iso-surface extraction are not robust enough for high percentages of outliers. In the current implementation of gridfit, the lowest Hausdorff distances (the ones stated in Table 1) for data sets with outliers were obtained for equally spaced grids. For further reduction of the Hausdorff distance, it is recommended to use L_1 splines, which perform significantly better for data sets with quite high percentages of outliers.

The time needed to calculate L_1 splines in their current implementation is high because one must solve a linear program, rather than a single linear least-squares system. However, the computing time of L_1 splines can be reduced by orders of magnitude by applying a domain decomposition procedure introduced in (Lin et al., 2006) as well as by using adaptive triangular grids.

4 CONCLUSIONS

There is an urgent need for accurate approximation of irregular, 3D data in urban terrain as well as in geometric modeling of irregular objects in general. The Hausdorff metric is a widely recognized, orientation-independent tool for measuring the accuracy of 3D reconstruction. The figures in Sec. 3 illustrate the correlation between lower Hausdorff distance and better reconstruction in the view of the user interested in practical applications.

The four procedures described in this paper all produced acceptable reconstructions for data sets without outliers. However, once there is a significant number of outliers in the data, L_1 splines yield the best results. Once implemented in a computationally efficient domain-decomposition framework and on more flexible triangular grids, L_1 splines will be computationally competitive with the other methods.

In the future, we will compare the procedures investigated in this paper with a wider class of reconstruction procedures and will integrate these procedures into complete reconstruction and texturing procedures that go all the way from the camera or other sensors to the textured model.

ACKNOWLEDGEMENTS

We express our appreciation to Michael Kazhdan and John D'Errico for them placing their well written and well commented source codes for iso-surface extraction and gridfit, respectively, on the Internet.

REFERENCES

Amenta, N., Choi, S., Dey, T. K., and Leekha, N. (2000). A simple algorithm for homeomorphic surface reconstruction. In *International Journal of Computational Geometry and Applications*, pages 213–222.

Baddeley, A. (1992). An error metric for binary images. In *Robust Computer Vision: Quality of Vision Algorithms, Proceedings, International Workshop on Robust Computer Vision*, pages 59–78.

Boissonnat, J., Cohen-Steiner, D., Mourrain, B., Rote, G., and Vegter, G. (2006). *Meshing of surfaces, effective computational geometry for curves and surfaces*. Mathematics and Visualization. Springer.

Bulatov, D. and Lavery, J. (2009). Comparison of reconstruction and texturing of 3d urban terrain by l_1 splines, conventional splines and alpha-shapes. In *Proc. Internat. Conf. Computer Vision Th. Applic VISAPP*, pages 403–409.

Bulatov, D. and Lavery, J. (to appear 2010). Reconstruction and texturing of 3d urban terrain from uncalibrated monocular images using l_1 splines. Photogr. Engr. and Remote Sensing.

D'Errico, J. (2006). Surface fitting using gridfit. `http://www.mathworks.com/matlabcentral/fileexchange/8998`.

DiBenedetto, E. (2002). *Real Analysis*. Birkhäuser Boston Inc.

Eck, M. and Hoppe, H. (1996). Automatic reconstruction of b-spline surfaces of arbitrary topological type. In *Proc. 23rd Annual Conf. Computer Graphics and Interactive Techniques*, pages 325–334.

Edelsbrunner, H. and Mücke, E. P. (1994). Three-dimensional alpha shapes. *ACM Trans. Graph.*, 13(1).

Guthe M., Borodin P., K. R. (2005). Fast and accurate hausdorff distance calculation between meshes. In *J. WSCG*, pages 41–48.

Haala N., B. C. (1998). Interpretation of urban surface models using 2d building information. In *Computer Vision and Image Understanding*, pages 204–214.

Heipke, C., Mayer, H., Wiedemann, C., and Jamet, O. (1997). Evaluation of automatic road extraction. In *In: International Archives of Photogrammetry and Remote Sensing*, pages 47–56.

Hoppe, H., DeRose, T., Duchamp, T., McDonald, J., and Stuetzle, W. (1992). Surface reconstruction from unorganized points. In *SIGGRAPH '92: Proceedings of the 19th annual conference on Computer graphics and interactive techniques*, pages 71–78. ACM.

Kazhdan, M. (2005). Reconstruction of solid models from oriented point sets. In *SGP '05: Proceedings of the third Eurographics symposium on Geometry processing*, pages 73–82.

Lavery, J. E. (2001). Shape-preserving, multiscale interpolation by bi- and multivariate cubic l1 splines. *Computer Aided Geometric Design*, 18(4):321–343.

Lin, Y.-M., Zhang, W., Wang, Y., Fang, S.-C., and Lavery, J. (2006). Computationally efficient models of urban and natural terrain by non-iterative domain decomposition with l_1 smoothing splines. In *Proceedings of the 25th Army Science Conference*.

Lorensen, W. E. and Cline, H. E. (1987). Marching cubes: A high resolution 3d surface construction algorithm. *SIGGRAPH Comput. Graph.*, 21(4):163–169.

Mayer H., B. J. (2006). Automated 3d reconstruction of urban areas from networks of wide-baseline image sequences. In *International Archives of the Photogrammetry, Remote Sensing and Spatial Information Sciences 37*, pages 633–638.

Olson, C. F. and Huttenlocher, D. P. (1997). Automatic target recognition by matching oriented edge pixels. *IEEE Transactions on Image Processing*, 6:103–113.

Seitz, S. M., Curless, B., Diebel, J., Scharstein, D., and Szeliski, R. (2006). A comparison and evaluation of multi-view stereo reconstruction algorithms. In *CVPR '06: Proceedings of the 2006 IEEE Computer Society Conference on Computer Vision and Pattern Recognition*, pages 519–528. IEEE Computer Society.